Supporting Information

Stable and Twisted 5,6:12,13-Dinaphtozethrene from Angular π-Extension

Jinlian Hu, [a] Qin Xiang, [a] Jun Xu,[b] Zhanqiang Xu,[*a] Guang Chen[*c] and Zhe Sun[*a]

[a.]*Institute of Molecular Plus, Tianjin Key Laboratory of Molecular Optoelectronic Sciences, Tianjin university 92 Weijin Road, Tianjin 300072, China*

[b.]*Health Science Platform, Tianjin University 92 Weijin Road, Tianjin 300072, China.*

[c]*Shaanxi Key Laboratory of Chemical Additives for Industry, Key Laboratory of Chemical Additives for China National Light Industry, College of Chemistry and Chemical Engineering, Shaanxi University of Science and Technology, Xi'an 710021, China.*

Table of Contents

1.Experimental section

1.1 General

All reagents were commercial available and used as received. Anhydrous THF was used by treatment with a solvent purification system. Dichloromethane (DCM) was dried over CaH_2 overnight and further distilled prior to use. All reactions were performed under argon atmosphere. Column chromatography was performed with silica gel (200-300 mesh). Gel permeation chromatography (GPC) isolation was performed on LaboACE LC-5060 with DCM as the eluent. Proton (^1H) NMR and carbon (^{13}C) NMR spectra were recorded on JEOL (JNM-ECZ600R/S1) 600 NMR spectrometer with tetramethylsilane (TMS) as the internal standard. Chemical shifts were assigned in ppm relative to residue protons ($CDCl_3$: 7.26 for ^1H, 77.16 for ^{13}C; toluene-d_8: 2.08, 6.97, 7.01, 7.09 for ^1H). The following abbreviations were used for multiplicities: s = singlet, d = doublet, t = triplet, m = multiplet. High resolution electrospray ionization (ESI) mass spectra were performed on Bruker MicrOTOF-Q II instrument. UV-vis-NIR absorption spectra were recorded on SHIMADZU UV-2600 spectrophotometer in toluene. The electrochemical measurements were carried out in anhydrous DCM containing $^nBu_4NPF_6$ as supporting electrolyte at a scan rate of 50 mV/s at room temperature under argon atmosphere by CHI 620E electrochemical analyzer. A three-electrode system with glassy carbon as working electrode, $Ag/AgNO_3$ as reference electrode, Pt wire as counter electrode was applied. The potential was calibrated against ferrocene/ferrocenium couple. The diffraction data were collected on XtaLAB Synergy diffractometer equipped with Hypix6000HE detector using a single-wavelength X-ray source. The ESR spectra were obtained on a JES-FA200 spectrometer. The VT ESR data were fitted with Bleaney-Bowers equation:[1]
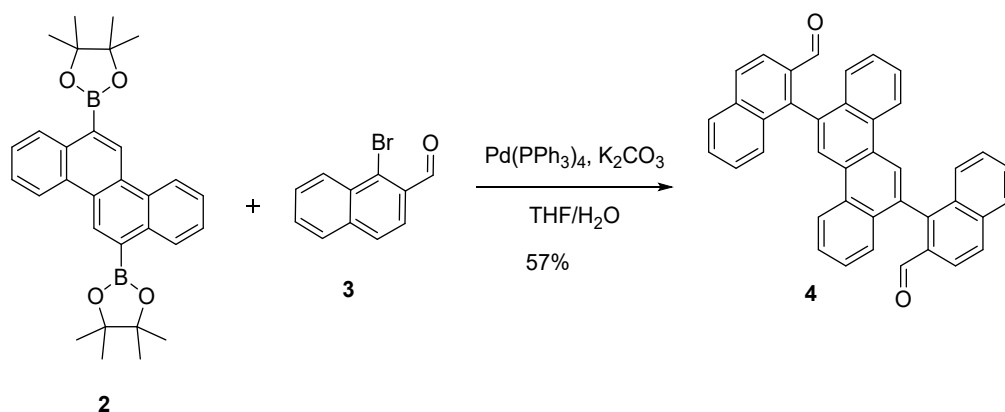
$$IT = \frac{C}{k_B[3 + exp(-2J/k_BT)]}$$

where, I is the ESR intensity, C is a constant, k_B is Boltzmann constant, and $-2J$ is correlated to the energy gap between the singlet ground state and the triplet excited

state.

1.2 Synthesis

Synthesis of Compound 4：

Compound **2** (340.0 mg, 0. 71 mmol), **3** (410.0 mg, 1.75 mmol), K_2CO_3 (483.7 mg, 3.50 mmol) and $Pd(PPh_3)_4$ (270.0 mg, 0.02 mmol) were dissolved in THF (25.0 mL)/H_2O (5.0 mL) mix solvent and the reaction mixture was purged with argon for 30 min. Then, it was heated to 90 ℃ under argon. After 48 h, the mixture was cooled to room temperature and the resulting suspension was filtered and washed with diethyl ether. The combined filtrates were concentrated under reduced pressure and purified on a silica-gel column chromatography (hexane/CH_2Cl_2 = 5/1, v/v) to give 200.0 mg of **4** in 57% yield as a yellow solid. ^1H NMR (600 MHz, $CDCl_3$): δ ppm 9.83 (d, J = 8.5 Hz, 2H), 8.82 (s, 2H), 8.73 (d, J = 8.5 Hz, 2H), 8.19 (dd, J = 8.6, 2.9 Hz, 2H), 8.06 (d, J = 8.7 Hz, 2H), 7.98 (d, J = 8.1 Hz, 2H), 7.64 – 7.55 (m, 4H), 7.49 (d, J = 8.4 Hz, 2H), 7.35 (m, 6H). ^{13}C NMR (150 MHz, $CDCl_3$): δ ppm 191.42, 143.57, 135.21, 131.74, 131.41, 129.13, 127.93, 127.39, 126.79, 126.56, 126.46, 126.31, 126.17, 123.48, 122.40, 121.29. HRMS (ESI) m/z [M+Na]$^+$ calcd for $C_{40}H_{24}NaO_2$ 559.1669, found 559.1672.

Synthesis of Compound 1：
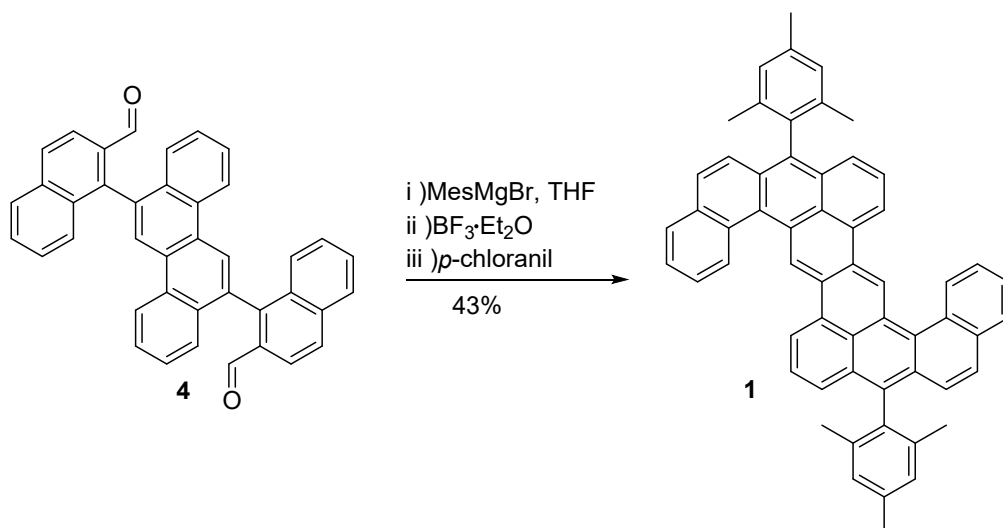
Compound **4** (50.0 mg, 0.09 mmol) was dissolved in 20.0 mL of dry THF under argon atmosphere. Then, mesitylmagnesium bromide in ether (1 M, 0.90 mL, 0.90 mmol) was added dropwise to the above solution and the mixture was stirred at room temperature for 2 hours. Subsequently, the reaction mixture was poured into 100 mL water and the crude product was extracted by chloroform. The obtained organic layer was dried over Na_2SO_4 and the solvent was removed under reduced pressure. The residue was then redissolved in 25.0 mL dry DCM under argon atmosphere and 2.5 mL of $BF_3 \cdot Et_2O$ was added. The mixture was stirred for 10 minutes and then washed with saturated $NaHCO_3$ solution (3 × 50.0 mL) and water (3 × 50.0 mL). The organic layer was dried over Na_2SO_4 and the solvent was removed under reduced pressure. The residue was redissolved in 20.0 mL dry toluene under argon atmosphere and *p*-chloranil in toluene (22.0 mg, 0.093mmol) was added dropwise. Upon addition of *p*-chloranil, the color of the reaction mixture changed slowly from light green to dark blue, and the reaction was monitored by TLC until completion. After evaporation of the solvent, the residue was purified by column chromatography (hexane/chloroform = 3/1, v/v) to give compound **1** (28.0 mg, 43% in three steps) as a dark-blue solid. ^{1}H NMR (600 MHz, CDCl$_3$): δ ppm 8.86 (s, 1H), 8.73 (d, *J* = 7.6 Hz, 2H), 8.33 (d, *J* = 7.4 Hz, 2H), 7.84 (d, *J* = 6.3 Hz, 2H), 7.62 (s, 2H), 7.53 (s, 2H), 7.46 (d, *J* = 9.2 Hz, 2H), 7.41 (s, 2H), 7.18 (d, *J* = 9.1 Hz, 2H), 7.12 (s, 4H), 2.47 (s, 6H), 1.85 (s, 12H). ^{13}C NMR (150 MHz, CDCl$_3$): δ

ppm 137.70, 137.25, 134.85, 134.65, 133.80, 132.52, 131.71, 131.04, 130.76, 130.30, 129.66, 129.13, 128.37, 128.08, 127.70, 127.46, 127.25, 126.89, 126.82, 125.81, 125.39, 124.72, 122.73, 120.91, 21.20, 20.05. HRMS (ESI) m/z [M]$^+$ calcd for $C_{58}H_{42}$ 738.3281 found 738.3260.

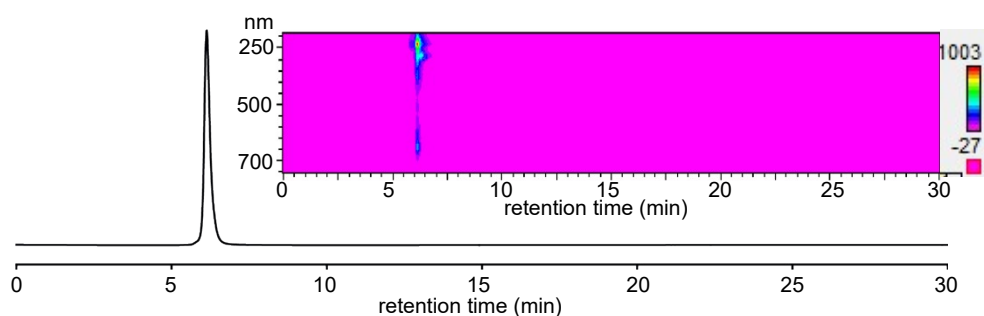## 2. Additional spectral data

2.1. HPLC analysis

Figure S1. HPLC analysis for **1** with Cosmosil 5C$_{18}$-MS-II column. Chromatographic conditions: flow rate = 0.5 mL/min, eluent = CH$_2$Cl$_2$, column temperature = 25 °C, detection = 254 nm. Inset: 2D-HPLC chromatograms.

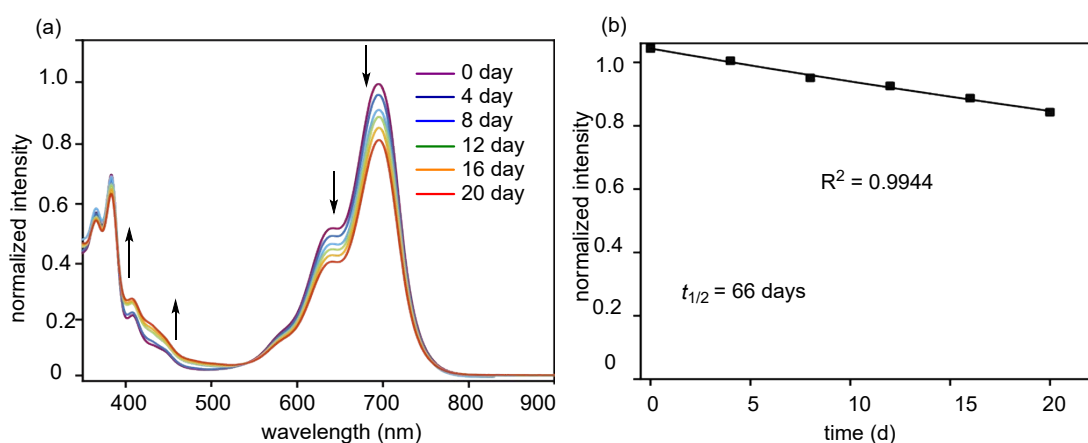### 2.2 Absorption intensity decay for stability test

Figure S2. (a) The UV-Vis-NIR absorption spectral changes of compound **1** in air saturated toluene under ambient light irradiation. (b) The plot of optical density decay and fitted with first-order kinetics
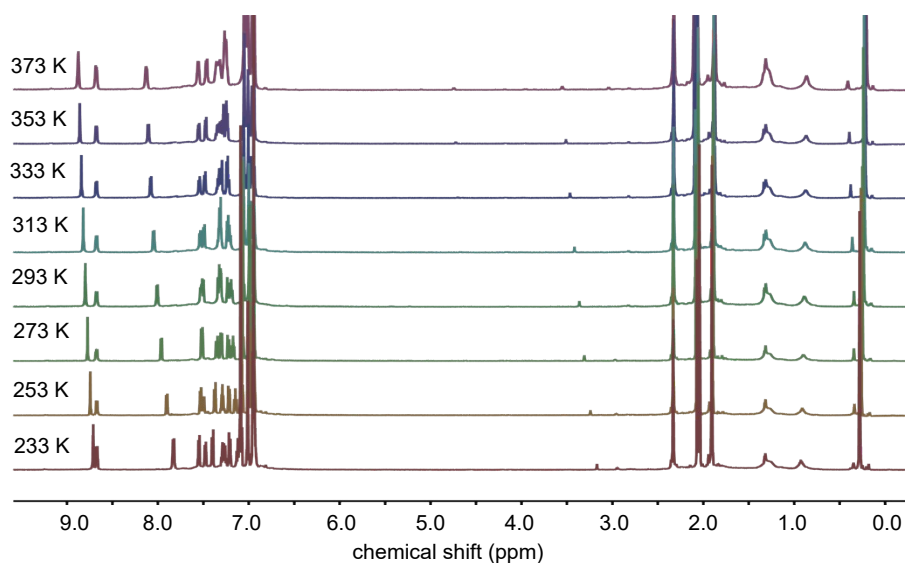
2.3 VT ¹H NMR spectra

Figure S3. Variable-temperature ^1H NMR spectra of **1** (toluene-d_8, 600 MHz).
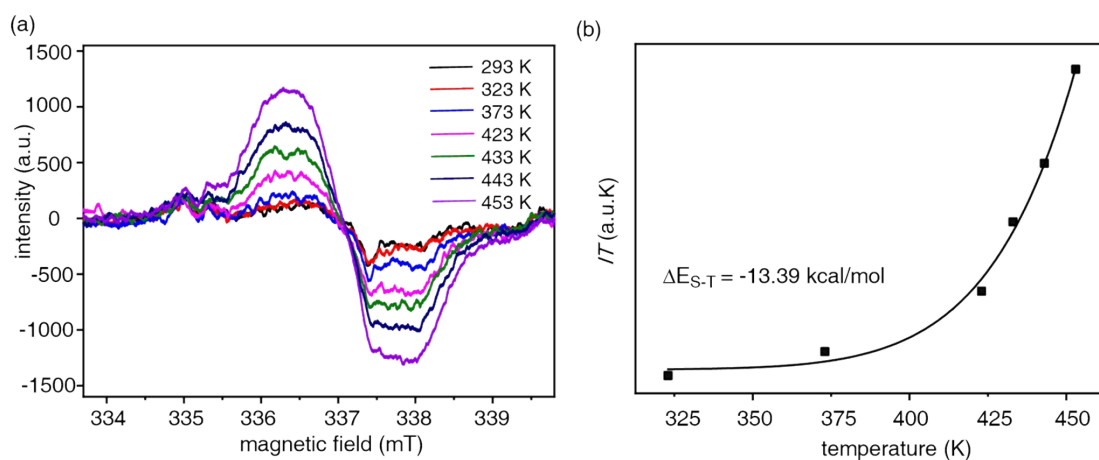
2.4 VT ESR spectra

Figure S4. (a) Variable-temperature ESR spectra of **1** from 293 K to 453 K and (b) fitted *IT-T* curve.

3. X-ray crystallographic data

Single crystals suitable for the X-ray analysis were obtained by slow diffusion of isopropanol to toluene for **1**. The single-crystal X-ray diffraction studies was carried out on the XtaLAB Synergy diffractometer using Cu Kα (λ = 1.54184 Å). The diffractometers are equipped with Hypix6000HE detector. The single crystal was

mounted using oil on a nylon loop fixed on a goniometer head and immediately transferred to diffractometer. The obtained diffraction data were processed by the program suite CrysAlispro (Rigaku Oxford Diffraction, CrysAlisPro Software system, version 1.171.40_64.53, Rigaku Corporation, Oxford, UK, 2019). The structure was solved with dual-space method using SHELXT program and refined with non-linear least square method using SHELXL program embedded in the program suite OLEX2. For more detailed information about diffraction data collection and refinement parameters, see Table S1 for **1.** The crystallographic data were deposited in Cambridge Crystallographic Data Centre (2090789). The data can be achieved free of charge from www.ccdc.cam.ac.uk/data_request/cif.

Table S1. Crystal data and structure refinement for **1** at 160 K.

Data deposition	CCDC 2090789
Empirical formula	$C_{65}H_{50}$
Formula weight	831.05
Temperature/K	160.0
Crystal system	monoclinic
Space group	$P2_1/c$
Unit cell dimensions	$a = 19.31790(10)$ Å
	$b = 11.15600(10)$ Å
	$c = 27.3475(2)$ Å
	$\alpha = 90°$
	$\gamma = 101.7070(10)°$
	$\gamma = 90°$
Volume/Å^3	5771.07(8)
Z	4
ρ_{calc}g/cm^3	0.956
μ/mm^{-1}	0.407
F (000)	1760
Crystal size/mm^3	0.25×0.15×0.05
Radiation	Cu Kα (λ = 1.54184)
Theta range for data collection/°	5.144 to 149.748
Index ranges	-23 $\leq$h $\leq$ 23, -13 $\leq$ k $\leq$ 13, -33 $\leq$ l $\leq$ 34
Reflections collected	201357
Independent reflections	11649 [R_{int} = 0.0705, R_{sigma} = 0.0176]
Data/restraints/parameters	11649/576/603
Goodness-of-fit on F^2	1.107
Final R indexes [I >= 2σ (I)]	R_1 = 0.0527, wR_2 = 0.1817
R indexes [all data]	R_1 = 0.0562, wR_2 = 0.1849
Largest diff. peak/hole /e Å^{-3}	0.21/-0.19

Table S2. The bond lengths of **1** in single crystal structure.
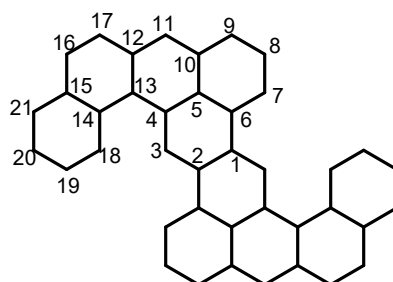
| Chemical bond	bond distance (Å)	Chemical bond	bond distance (Å)
C1-C2	1.439 (2)	C5-C10	1.445 (2)
C1-C6	1.471 (2)	C9-C10	1.395 (2)
C5-C6	1.413 (2)	C8-C9	1.369 (2)
C4-C5	1.419 (2)	C8-C7	1.404 (3)
C4-C3	1.444 (2)	C7-C6	1.368 (2)
C2-C3	1.351 (2)	C13-C14	1.444 (2)
C4-C13	1.412 (2)	C16-C14	1.408 (2)
C13-C12	1.448 (2)	C15-C16	1.454 (2)
C12-C11	1.378 (3)	C16-C17	1.328 (2)
C11-C10	1.419 (2)	C21-C20	1.399 (3)
C14-C18	1.424 (2)	C21-C15	1.389 (2)
C19-C18	1.369 (2)	C12-C17	1.371 (1)
C20-C19	1.382 (3)	C21-C20	1.399 (3)
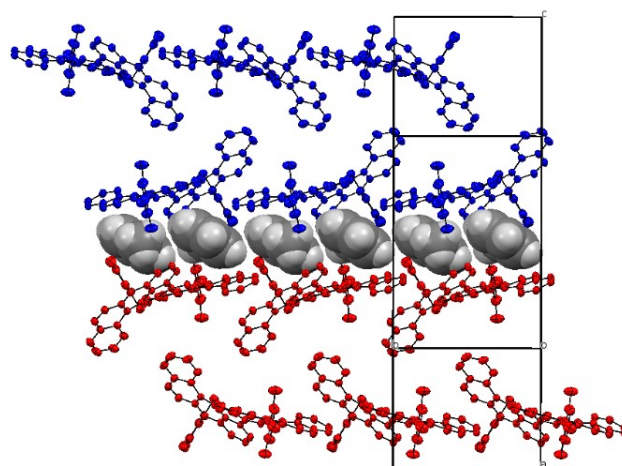
Figure S5 Packing structure with solvent molecules shown in space-filling model.

4. The theoretical calculation

4.1 General

Theoretical calculations were performed with the Gaussian09 package[2] using the density functional theory (DFT) method with Becke's three-parameter hybrid exchange functionals and the Lee-Yang-Parr correlation functional (B3LYP) employing the 6-31G (d,p) basis set for all atoms.[3-7] The geometry optimizations of **1** were conducted at UB3LYP/6-31G (d,p) level of theory. Time-dependent DFT (TD-DFT) was performed on fully optimized structure. All optimized structures were confirmed to be true minima by vibrational analysis with no imaginary frequency and all transition states were confirmed with one imaginary frequency. Diradical character indices (y_0) were determined by Yamaguchi scheme: $y_0 = 1-[2T/(1+T^2)]$, where T equal to [(n_{HONO}-n_{LUNO})/2].[8,9] n_{HONO} and n_{LUNO} represent the occupation number of the highest occupied natural orbital (HONO) and the occupation number of the lowest unoccupied natural orbital (LUNO), respectively, which were obtained by UCAM-B3LYP/6-31G (d,p) method. NICS values were obtained at the GIAO-UB3LYP/6-31G (d,p) level of theory with the optimized structure.

4.2 TD-DFT calculation

Table S3. Calculated electronic transitions for **1**.

No.	Energy (eV)	Wavelength (nm)	Oscillator Strength	Major Contributions
1	1.5799	784.78	0.8826	HOMO→LUMO (99%)
2	2.6856	461.67	0.0180	HOMO-1→LUMO (48%), HOMO→LUMO+1 (44%)
3	2.7116	457.23	0.0035	HOMO-2→LUMO (56%), HOMO→LUMO+2 (40%)
4	2.8903	428.96	0.0010	HOMO-3→LUMO (37%), HOMO→LUMO+3 (52%)
5	2.9976	413.61	0.4551	HOMO-2→LUMO (40%), HOMO→LUMO+2 (56%)
6	3.0374	408.20	0.0004	HOMO-5→LUMO (32%), HOMO-4→LUMO (18%), HOMO-3→LUMO (6%), HOMO→LUMO+4 (40%),

4.3 NICS(1)zz calculation
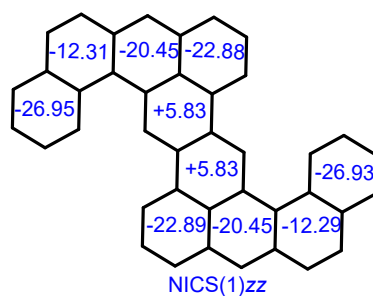
Figure S6. NICS(1)zz values for **1** at UB3LYP/6-31G (d, p) level of theory.

4.4 Molecular orbital profiles and spin density distribution
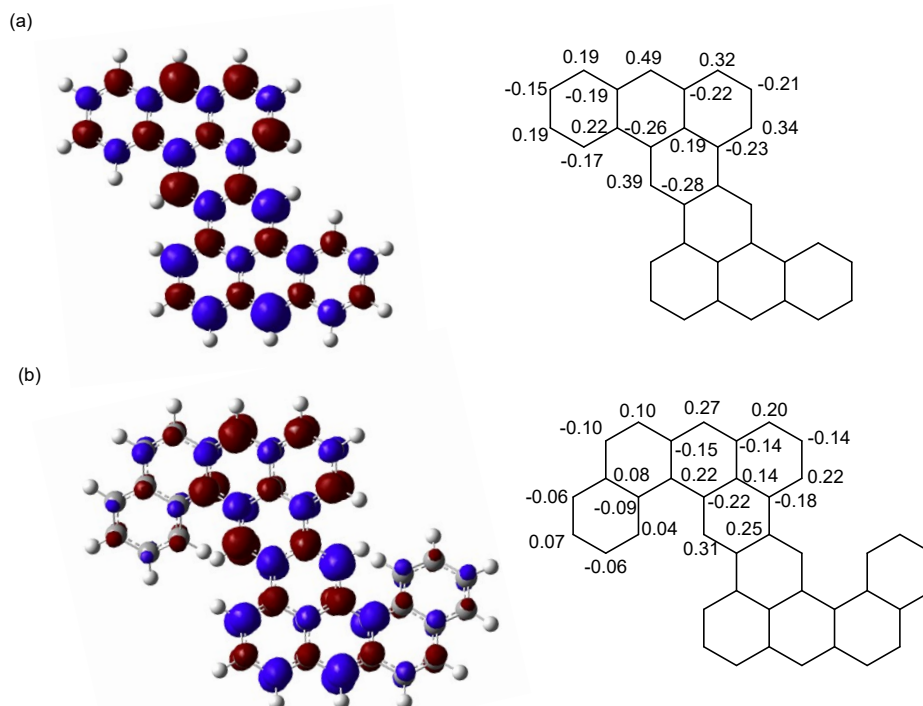

Figure S7. Calculated spin density distribution and Mulliken spin density (msd) values for (a) 5,6:12,13-dibenzozethrene, (b) 5,6:12,13-dinaphtozethrene at UCAM-B3LYP/6-31G (d, p) level of theory.
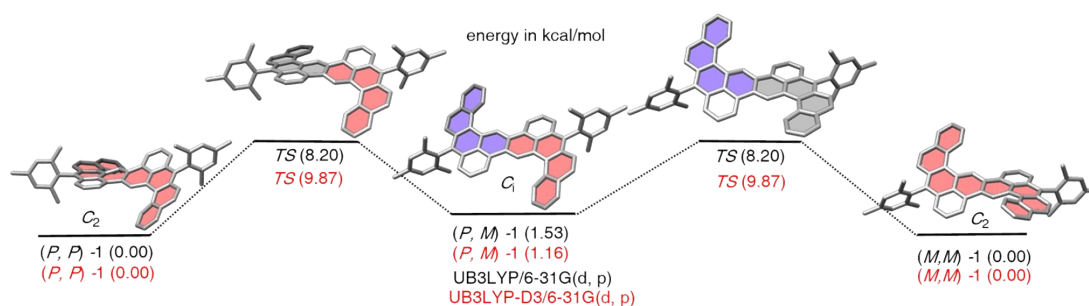
4.5 Energy profile for isomerization

Figure S8. Energy profile for isomerization among (*P, P*)-**1**, (*P, M*)-**1** and (*M, M*)-**1** at UB3LYP/6-31G (d, p) and UB3LYP-D3/6-31G (d, p) level of theory.

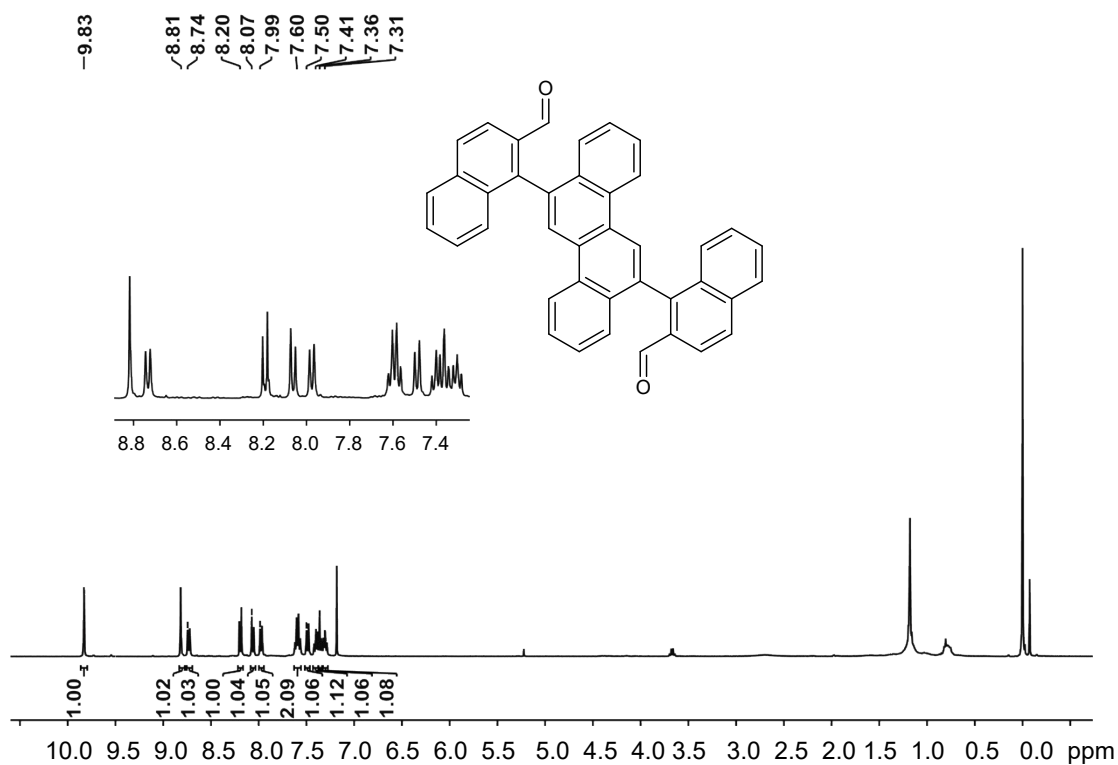# 5. ¹H/¹³C NMR and MS spectra for new compounds

Figure S9. ¹H NMR spectrum of compound **4** in CDCl₃ (298 K, 600 MHz).

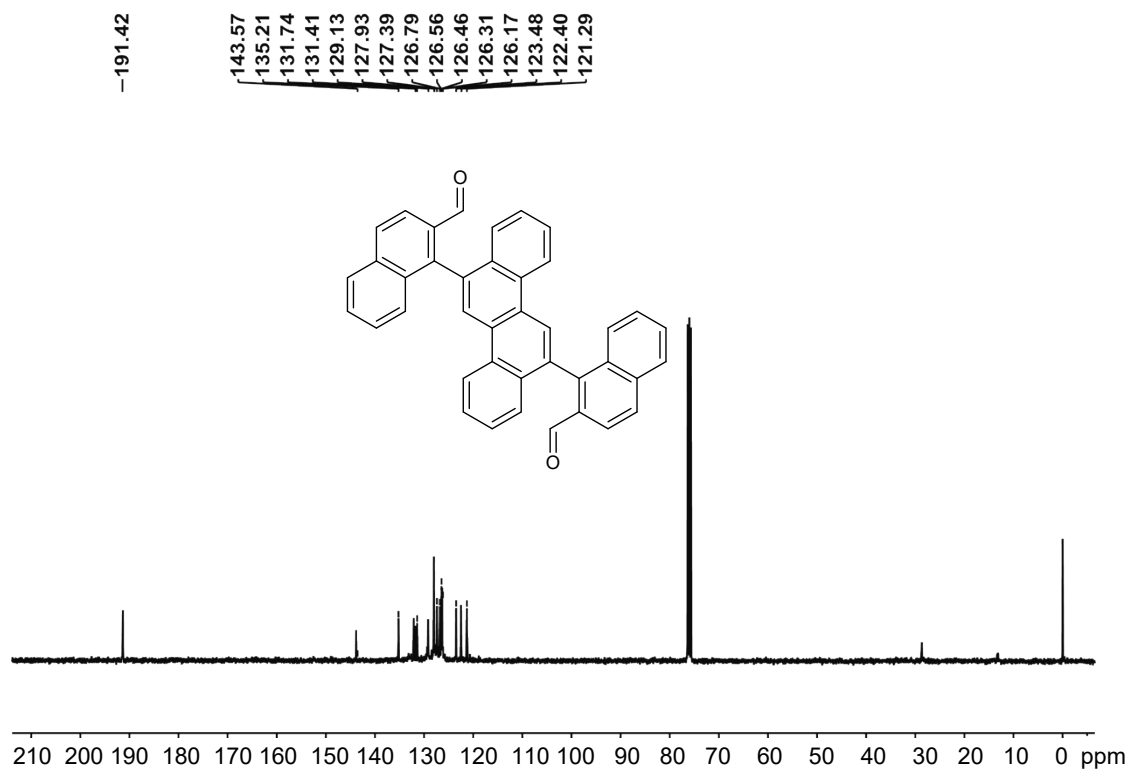**Figure S10.** ^{13}C NMR spectrum of compound **4** in CDCl$_3$ (298 K, 600 MHz).

Evaluation Spectra / Validation Formula:

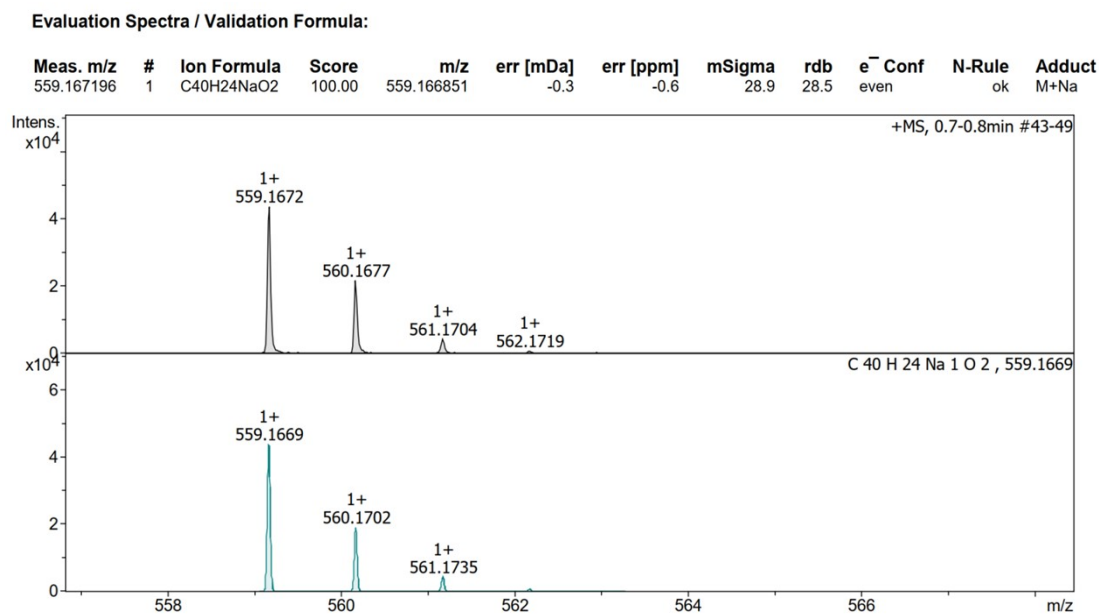| Meas. m/z	#	Ion Formula	Score	m/z	err [mDa]	err [ppm]	mSigma	rdb	e⁻ Conf	N-Rule	Adduct
559.167196	1	C40H24NaO2	100.00	559.166851	-0.3	-0.6	28.9	28.5	even	ok	M+Na

Figure S11. HR-ESI MS spectrum of compound **4**.

Figure S12. ^1H NMR spectrum of compound **1** in CDCl$_3$ (298 K, 600 MHz).

13

Figure S13. ^{13}C NMR spectrum of compound **1** in CDCl$_3$ (298 K, 600 MHz).
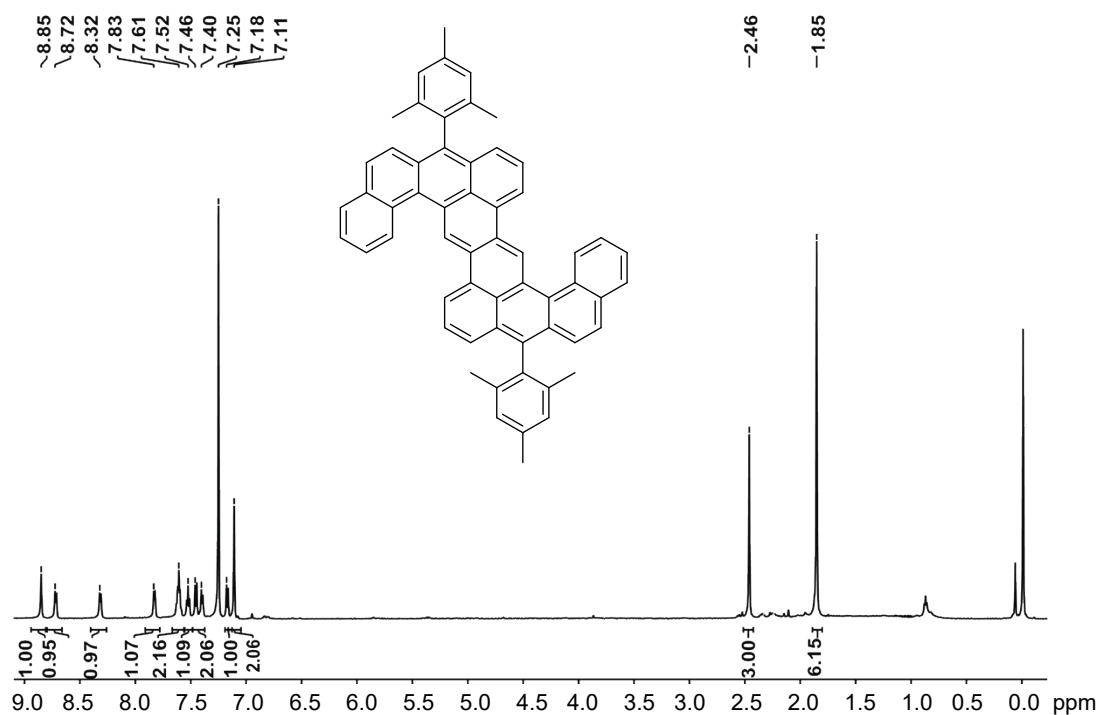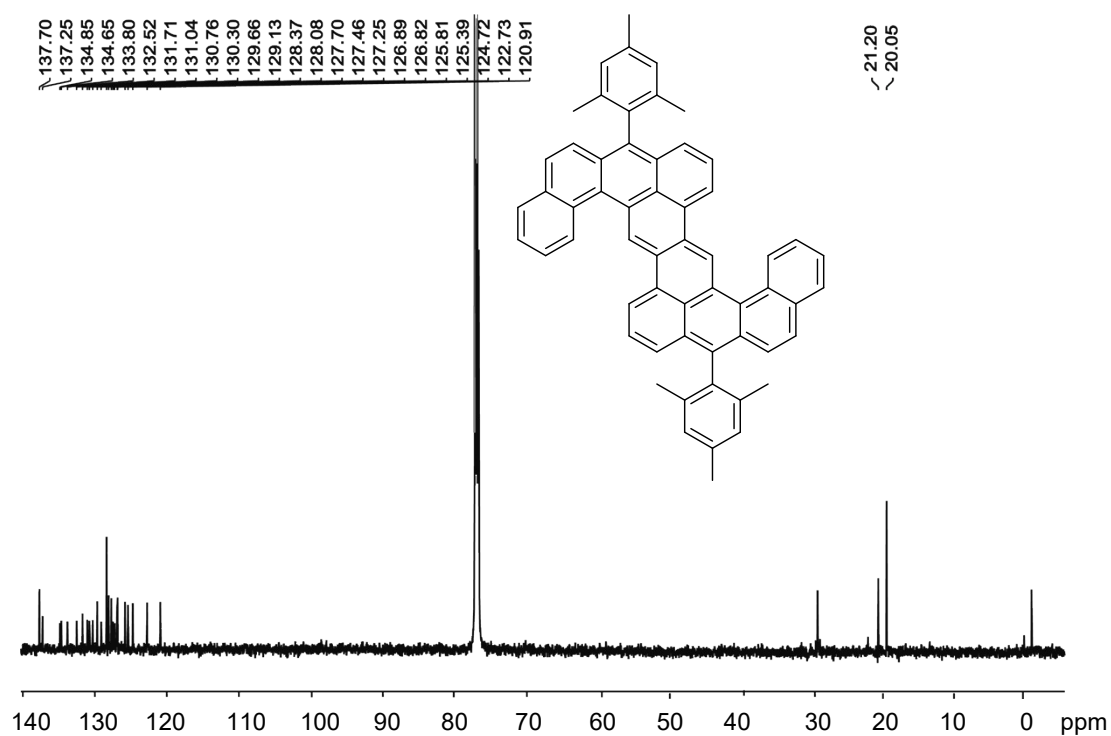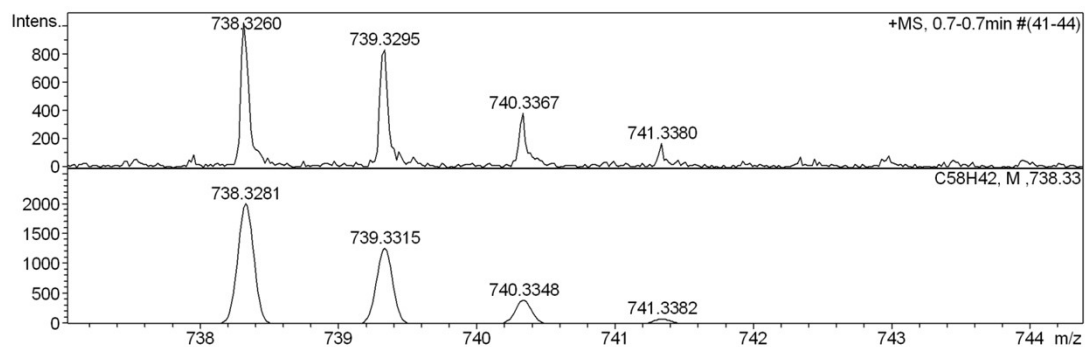

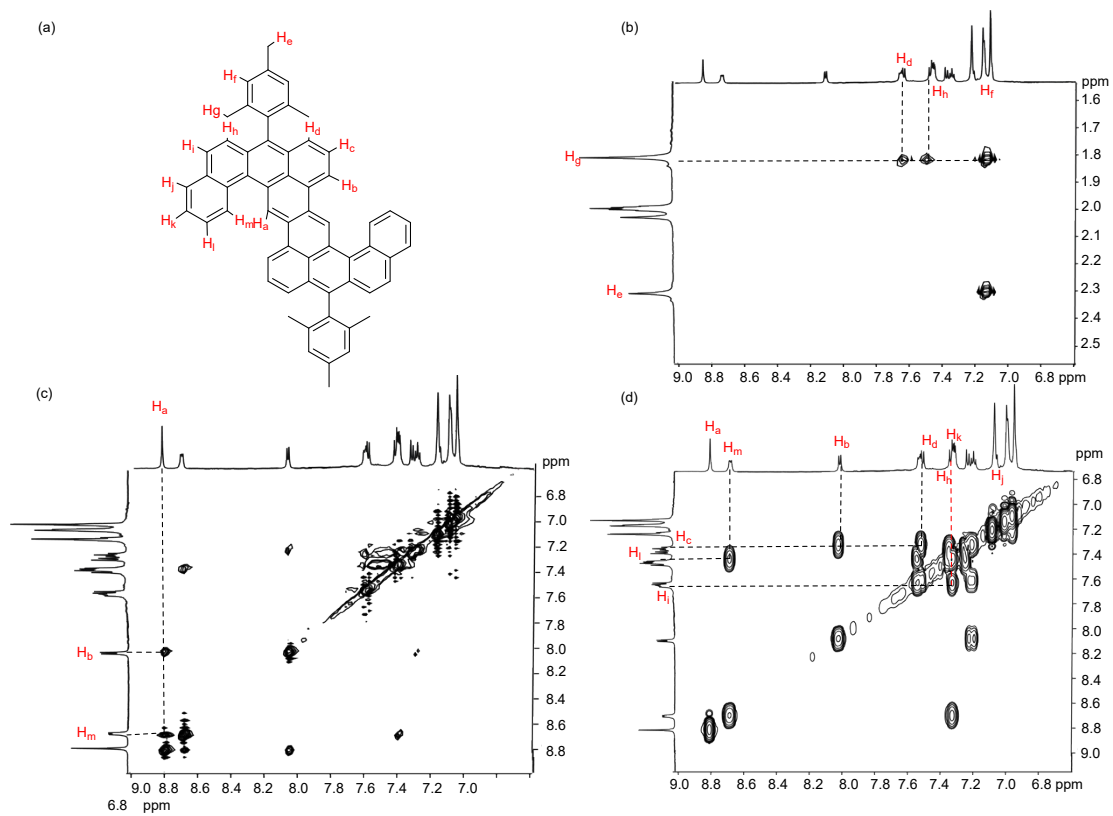**Figure S14.** HR-ESI MS spectrum of compound **1**.

Figure S15. (a) Chemical structure of **1**, (b) aliphatic region, (c) aromatic region of ^{1}H-^{1}H NOSEY NMR spectrum and (d) ^{1}H-^{1}H COSY NMR spectrum of **1** (toluene-d_8, 600 MHz).

6. References

1. B. Bleaney, K. D. Bowers, *Proc. R. Soc. London Ser. A*, 1952, **214**, 451 – 465.

2. Gaussian 09, Revision E.01. M. J. Frisch, G. W. Trucks, H. B. Schlegel, G. E. Scuseria, M. A. Robb, J. R. Cheeseman, G. Scalmani, V. Barone, B. Mennucci, G. A. Petersson, H. Nakatsuji, M. Caricato, X. Li, H. P. Hratchian, A. F. Izmaylov, J. Bloino, G. Zheng, J. L. Sonnenberg, M. Hada, M. Ehara, K. Toyota, R. Fukuda, J. Hasegawa, M. Ishida, T. Nakajima, Y. Honda, O. Kitao, H. Nakai, T. Vreven, J. A. Montgomery, Jr., J. E. Peralta, F. Ogliaro, M. Bearpark, J. J. Heyd, E. Brothers, K. N. Kudin, V. N. Staroverov, T. Keith, R. Kobayashi, J. Normand, K. Raghavachari, A. Rendell, J. C. Burant, S. S. Iyengar, J. Tomasi, M. Cossi, N. Rega, J. M. Millam, M. Klene, J. E. Knox, J. B. Cross, V. Bakken, C. Adamo, J. Jaramillo, R. Gomperts, R. E. Stratmann, O. Yazyev, A. J. Austin, R. Cammi, C. Pomelli, J. W. Ochterski, R. L. Martin, K. Morokuma, V. G. Zakrzewski, G. A. Voth, P. Salvador, J. J. Dannenberg, S. Dapprich, A. D. Daniels, O. Farkas, J. B. Foresman, J. V.Ortiz, J. Cioslowski, and D. J. Fox, Gaussian, Inc., Wallingford CT, 2013.

3. A. D. Becke, *J. Chem. Phys.* 1993, **98**, 5648-5652.

4. C. Lee, W. Yang, R. G. Parr, *Phys. Rev. B: Condens. Matter Mater. Phys.* 1988, **37**, 785-789.

5. R. Ditchfield, W. J. Hehre, J. A. Pople, *J. Chem. Phys.* 1971, **54,** 724-728.

6. W. J. Hehre, R. Ditchfield, J. A. Pople, *J. Chem. Phys.* 1972, **56**, 2257-2261;

7. P. C.Hariharan, J. A. Pople, *Theor. Chim. Acta*. 1973, **28**, 213-222.

8. S. Yamanaka, M. Okumura, M. Nakano and K. Yamaguchi, *J. Mol. Struct.* 1994, **310**, 205.

9. K. Kamada, K. Ohta, A. Shimizu, T. Kubo, R. Kishi, H. Takahashi, E. Botek, B. Champagne and M. Nakano, *J. Phys. Chem. Lett.* 2010, **1,** 937